The *Herschel* SPIRE Spectrometer Phase Correction Data Processing Tasks

Trevor Fulton[a], David A. Naylor[a], Ed Polehampton[a,b], Rosalind Hopwood[c], Ivan Valtchanov[d], Nanyao Lu[e], Nicola Marchili[f], Jeremy Zaretski[g]

[a]Department of Physics and Astronomy, University of Lethbridge, Lethbridge, Alberta, Canada
[b]Rutherford Appleton Laboratory, Chilton, Oxfordshire, United Kingdom
[c]Imperial College, London, United Kingdom
[d]Herschel Science Centre, Madrid, Spain
[e]NASA Herschel Science Centre, Pasadena, California, USA
[f]Universitá di Padova, Padova, Italy
[g]Blue Sky Spectroscopy, Lethbridge, Alberta, Canada

Introduction

The Spectral and Photometric Imaging Receiver (SPIRE) Fourier Transform Spectrometer (FTS) is a sub-millimetre imaging spectrometer that operated on board the *Herschel* Space Observatory between May 2009 and April 2013 (Pilbratt 2010, Griffin 2010). The SPIRE FTS contains two bolometer detector arrays that cover the frequency range from 447 to 1546 GHz (671 to 194 μm). Interferograms are produced by scanning the spectrometer mechanism (SMEC) – the moving mirror that modulates the optical path difference (OPD).

The power measured in the image plane of the FTS should strictly depend on the difference between the optical path lengths of the two beams of the interferometer. The measured interferograms should possess even symmetry with respect to zero path difference (ZPD) – the unique point where the path lengths of the two beams are identical and constructive interference occurs for radiation at all frequencies. The recorded interferograms are not perfectly symmetric for several reasons, which include random noise, discrete sampling, dispersive elements within the interferometer, non-linear detector response, read-out electronics, and thermal inertia of the detectors (Swinyard 2014, Naylor 2014). The degree of this asymmetry is referred to as a phase, $\phi_i(\nu)$.

Time Domain Phase Correction

The detector and read-out electronics that convert the analog detector signals into a digital, computer-readable format introduce a frequency-dependent phase that will, in general, be non-linear. The thermal response of the bolometers introduces an additional component. The overall non-linear phase, $\phi_{Electrical\text{-}i}(\nu)$, unique to each detector i, manifests as a time delay on the order of 10-30 ms imparted to the recorded detector signals, $V_i(t)$ (see panels B and D).

If left uncorrected, the time delay imparted to the detector signals results in a 20-60 μm shift in position when the timeline signals are converted to interferograms ($V_i(x)$) (see panels C, E and transition A→B→C). The time delay will correspond to either a forward or a negative position shift with respect to ZPD, depending on the direction of motion of the FTS mirror for that scan (see panel C). The Time Domain Phase Correction step computes this detector-specific electrical phase, $\phi_{Electrical\text{-}i}(\nu)$, and corrects the timelines by way of convolution with the inverse transform of this phase (see transition A→D). This has the effect of correcting the position shifts in the resultant interferograms (see transition D→E).

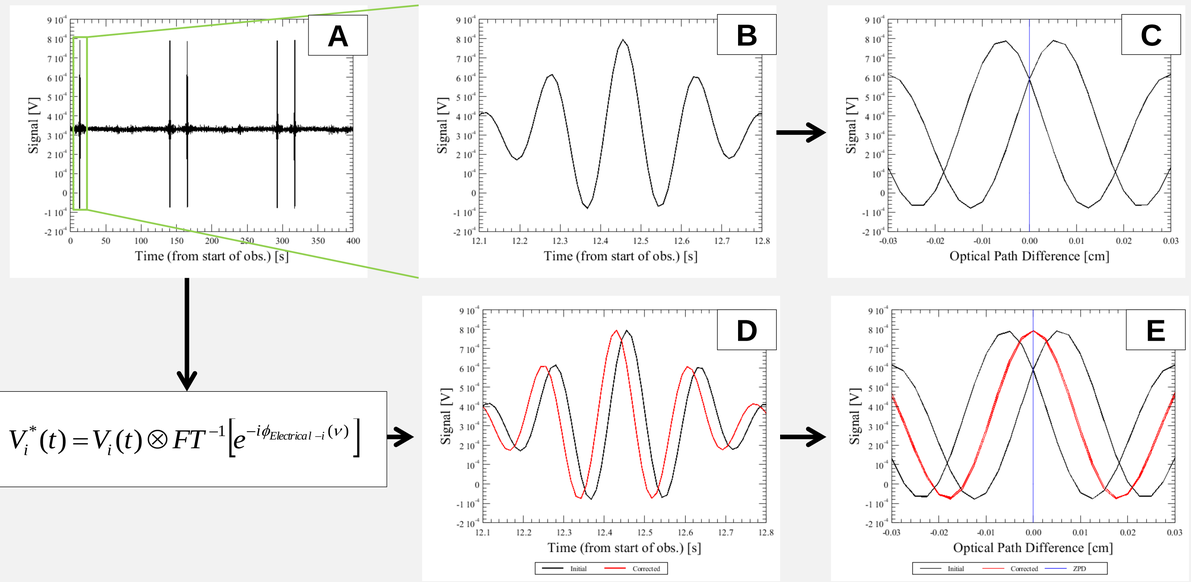

$$V_i^*(t) = V_i(t) \otimes FT^{-1}\left[e^{-i\phi_{Electrical-i}(\nu)}\right]$$

Interferogram Phase Correction

The remaining phase components are best corrected in the spatial domain where the recorded signals are a function of mirror position, $V_i(x)$. Regardless of resolution mode, the phase at this stage can be characterized by the double-sided portion of the measured interferograms ($V_{DS\text{-}i}(x)$, shown in blue below) and subsequently removed from the data (Forman 1966).

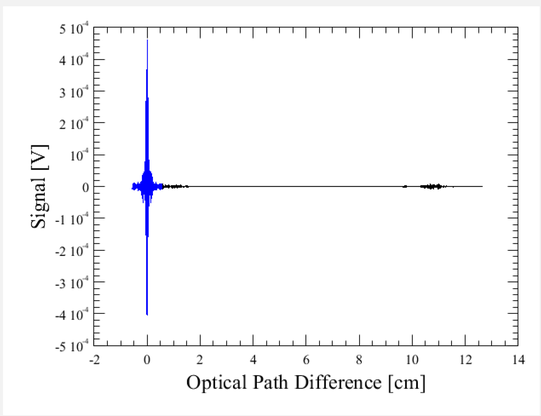

$$\phi_{DS-i}(\nu) = \mathrm{Tan}^{-1}\left[\frac{\mathrm{Im}\left(V_{DS-i}(\nu)\right)}{\mathrm{Re}\left(V_{DS-i}(\nu)\right)}\right]$$

Fitted Polynomial

The first iteration of the phase correction algorithm involved fitting a low-order polynomial to the measured in-band phase of each interferogram. The measured interferograms were corrected by way of convolution with the inverse transform of the fitted phase.

$$\phi_{Fit-i}(\nu) = a_i + b_i(\nu) + c_i(\nu^2) + d_i(\nu^3) + e_i(\nu^4)$$
$$V_i^*(x) = V_i(x) \otimes FT^{-1}\left[e^{-i\phi_{Fit-i}(\nu)}\right]$$

Calibrated Phase

The next iteration of the phase correction algorithm involved the use of a fixed, or calibrated, non-linear phase. Analysis of the initial in-flight SPIRE FTS data showed that the phase-correction function required at the interferogram phase correction step was of a similar shape, for most observations. For each detector of the SPIRE FTS, a non-linear phase correction function was derived by combining the scans of all of the dark sky observations. Astronomical observation spectra, $V_i(\nu)$, were corrected by way of multiplication with the calibrated phase.

$$\phi_{CAL-i}(\nu) = \mathrm{Tan}^{-1}\left[\frac{\mathrm{Im}\left(\overline{V_{Dark-i}(\nu)}\right)}{\mathrm{Re}\left(\overline{V_{Dark-i}(\nu)}\right)}\right]$$
$$V_i^*(\nu) = V_i(\nu) \times e^{-i\phi_{CAL-i}(\nu)}$$

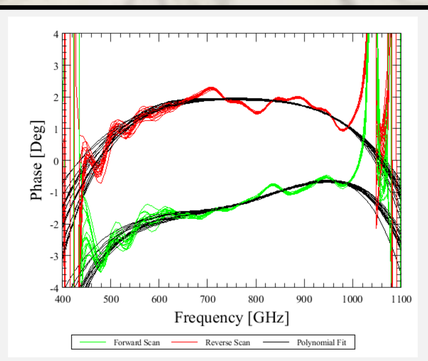

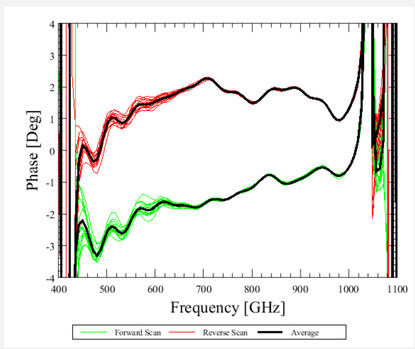

Hybrid Method

The current algorithm (Fulton 2014) is a combination of the first two algorithms. The non-linear portion of the phase, characterized by the double-sided portion of the average interferograms *for that observation*, is computed and removed. A linear function is then fit to any remaining phase and subsequently removed by convolution.

$$\phi_{NonLin-i}(\nu) = \mathrm{Tan}^{-1}\left[\frac{\mathrm{Im}\left(\overline{V_i(\nu)}\right)}{\mathrm{Re}\left(\overline{V_i(\nu)}\right)}\right]$$
$$V_i^*(\nu) = V_i(\nu) \times e^{-i\phi_{NonLin-i}(\nu)}$$
$$\phi_{Fit-i}(\nu) = a_i + b_i(\nu)$$
$$V_i^{**}(x) = V_i^*(x) \otimes FT^{-1}\left[e^{-i\phi_{Fit-i}(\nu)}\right]$$

Results

As shown below, the phase correction step produces interferograms that are symmetric about the position of ZPD.

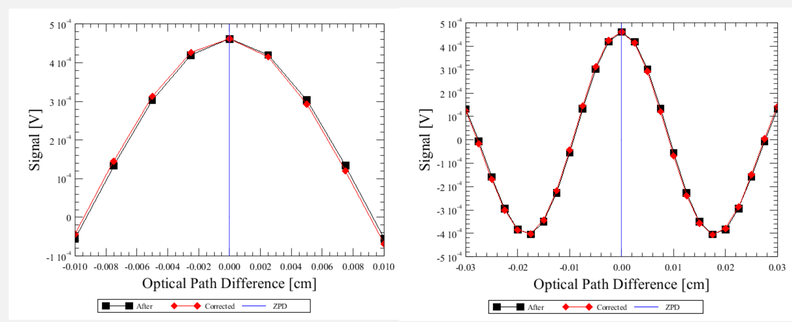

Conclusion

The phase correction algorithms for Herschel/SPIRE FTS data and their evolution have been presented. While developed specifically for the SPIRE FTS these techniques can be readily applied to data obtained with other infrared imaging Fourier transform spectrometers.

Acknowledgements The funding for the Canadian contribution to SPIRE is provided by the Canadian Space Agency and NSERC. Background image courtesy of ESA.

References

1. G. L. Pilbratt, et al., 2010, *Herschel Space Observatory. An ESA facility for far-infrared and submillimetre astronomy*, A&A, 518, L1;
2. M. J. Griffin, et al., 2010, *The Herschel-SPIRE instrument and its in-flight performance*, A&A, 518, L3;
3. B. Swinyard, et al., 2014, *Herschel/SPIRE Fourier Transform Spectrometer Calibration*, MNRAS, 440, 3658;
4. D. Naylor, et al., 2014, *In-orbit performance of the Herschel/SPIRE imaging Fourier transform spectrometer: lessons learned*. Proc. SPIE. 9143, Space Telescopes and Instrumentation 2014: Optical, Infrared, and Millimeter Wave, 91432D;
5. M. L. Forman, et al., 1966, *Correction of asymmetric interferograms obtained in Fourier transform spectroscopy*, J.O.S.A., 56, 59;
6. T. Fulton, et al., 2014, *The data processing pipeline for the Herschel SPIRE Fourier transform spectrometer*, A&A, in preparation.